Title	The Effects of Oil Property and Inclination Angle on Oil–Water Core Annular Flow Through U-Bends
Author(s)	Jiang, Fan; Wang, Ke; Skote, Martin; Wong, Teck Neng; Duan, Fei
Citation	Jiang, F., Wang, K., Skote, M., Wong, T. N., & Duan, F. (2017). The Effects of Oil Property and Inclination Angle on Oil–Water Core Annular Flow Through U-Bends. Heat Transfer Engineering, in press.
Date	2017
URL	http://hdl.handle.net/10220/44168
Rights	© 2017 Taylor & Francis Group, LLC. This is the author created version of a work that has been peer reviewed and accepted for publication by Heat Transfer Engineering, Taylor & Francis Group, LLC. It incorporates referee's comments but changes resulting from the publishing process, such as copyediting, structural formatting, may not be reflected in this document. The published version is available at: [http://dx.doi.org/10.1080/01457632.2017.1320168].

The effects of oil property and inclination angle on oil-water core annular flow through U-bends

Fan Jiang, Ke Wang, Martin Skote, Teck Neng Wong, Fei Duan

School of Mechanical and Aerospace Engineering, Nanyang Technological University, Singapore

Address correspondence to Dr. Martin Skote, School of Mechanical and Aerospace Engineering, Nanyang Technological University, 50 Nanyang, Avenue, Singapore 639798, Singapore. E-mail: mskote@ntu.edu.sg Tel: 65-67904271. Fax: 65-67924062

Fan Jiang received the M.S. and Ph.D. degrees in Mechanical Engineering from Central South University and South China University of Technology in 2003 and 2006, respectively. He is an associate professor in Mechanical Engineering at Guangzhou University and is visiting scholar at Huazhong University of Science and Technology, and he was a research fellow in numerical simulation at Nanyang Technological University (2013-2014). Current research focuses on computational fluid dynamics, environmental materials, and innovative design. He has published more than 50 papers in leading journals. He has received Science and Technology Progress Award of Guangdong Province in 2015, Teaching achievement award of Guangdong Province in 2014, and more than twenty national invention patents.

Ke Wang is a research fellow in Nanyang Technological University. He obtained his Ph.D. degree (Engineering Thermal Physics) from Xi'an Jiatong University in 2012. His research focus is on two phase flow and heat transfer, instability analysis, droplet entrainment, and bubble dynamics.

Martin Skote received his Master (1994) and Ph.D. (2001) degrees from the Royal Institute of Technology (KTH), Stockholm, in Mechanical Engineering with a focus on turbulence. He is since 2008 Assistant Professor in the School of Mechanical & Aerospace Engineering, Nanyang Technological University (NTU) in Singapore. His research interests include turbulent boundary layers, direct numerical simulations, flow control, insect flight, atmospheric flow and urban air quality. Prior to joining NTU, he worked for the Institute of High Performance Computing, where he developed a numerical tool for air pollution dispersion simulations in collaboration with the National Environment Agency in Singapore.

Teck Neng Wong is an associate professor at Nanyang Technological University. He obtained his Ph.D. degree from University of Strathclyde, Scotland in 1990. His research focus is on two-phase flow and heat transfer, multiphase flows in microfluidic channels, spray cooling, two-phase flow in evaporator and condenser.

Abstract

Understanding the impact mechanism of the oil properties and the bend geometric parameters on oil-water core annular flow in bends is of great importance for the design and operation of bend pipelines. To address this, the oil-water core annular flow through U-bends is analyzed numerically, by using the volume of fluid technique together with the continuum surface stress method. A good match is observed between the numerically simulated phase contours and those taken from reported experiments. The influence of the inclination angle, the inlet diameter ratio, oil properties, and the pipe materials on the hydrodynamics is investigated together with the fouling characteristics of core annular flows. Through the numerical simulations, the flow in a range of operating conditions has been determined, together with the influence of geometric parameters and pipe material.

INTRODUCTION

In the last decades, the water-lubricated transport of high viscous oil has become economical for the petroleum industry. With this technique, water surrounds the oil core located at the center, to form the core annular flow of oil and water. Due to its immense industrial importance, numerous works have been conducted to investigate different aspects of oil-water flow by utilizing experimental, analytical and numerical methods. Experimental studies have been reported by Charles et al. [1], Arney et al. [2], and Sotgia et al. [3] on horizontal core annular flow and by Parda and Bannwart [4], Rrodriguez et al. [5] on vertical upflow. Owing to its efficiency as a method to understand flow behavior in detail, a number of studies on numerical analysis of oil-water flow have been conducted in the past. Bai et al. [6] used a control volume method to simulate core annular flow, and then assumed an axisymmetric equal density wavy flow to predict wavelength, wave shape, pressure gradient and pressure distribution over the interface. Kao et al. [7] performed simulations of turbulent wavy liquid-liquid flow, and solved the turbulence kinetic energy and dissipation equations by using the shear stress transport (SST $k-\omega$) model, and subsequently found that the model prediction of pressure distribution and wavelength was better than that of the original $k-\omega$ model. Myungoo et al. [8] used a level set approach for capturing the interface between oil and water, and succeeded in predicting the spatially periodic waves which agreed with the experimental observations. However, the

majority of the research undertaken is either for a horizontal or a vertical direction of straight conduit, while flow through pipefittings has rarely been studied.

U-bends are a commonly encountered pipefitting in petroleum transportation, chemical system, refrigeration system and nuclear reactors. Many investigations have been performed on gas-liquid two-phase flow through return bends; these studies have proposed models to predict two-phase pressure drop in bends [9-13] while some works have reported the impact of return bend on the downstream flow patterns in case of air-water flow [14-20]. However, studies in U-bends for oil-water two-phase flow are relatively few. Sharma et al. [21,22] experimentally investigated the oil-water flow through return bends, and they noticed that the bend geometry influences the downstream flow regimes. In addition, they compared the pressure drop under different bend geometry, and proposed an expression of two-phase bend loss coefficients. Sumana et al. [23] used FLUENT software to simulate the core annular flow of lubricating oil and water in return bends, and the numerical phase distribution matched well with that recorded from experiments. Moreover, they obtained the profiles of velocity, pressure, and volume fraction, and they also discussed the fouling tendency. However, to our best knowledge, there is no previous work dedicated to understand the effects of oil properties, bend geometric parameters, and pipe material on oil-water core annular flow through U-bends.

In this study, oil-water flow in U-bends is simulated using the same fluid pair through the same geometry as mentioned by Sharma et al. [21,22]. Such an effort is expected to extend the

study with the effects of oil property and inclination angle on oil-water core annular flow through U-bend. Through this work, the reason behind the observed increasing pressure drop is revealed, and the means to avoid the oil adhering to pipe wall are obtained. These results are expected to be useful for designing pipeline networks, and can help us determine the optimal range of operating conditions, such as the geometric parameters and pipe material. In addition, the independence of the choice of turbulence model is discussed.

MATHEMATICAL MODELING

Numerical simulation models for multiphase flow are commonly divided into Eulerian-Lagrangian and Eulerian-Eulerian approach. Relative to Eulerian-Lagrangian model, the Eulerian-Eulerian model can simulate the separated flow with relatively well-defined interface. Considering the hydrodynamics of oil-water flow [23], an Eulerian-Eulerian model based on the Volume of Fluid (VOF) technique in FLUENT is suitable for the current work. Note that the full governing equations (Navier-Stokes) cannot be solved directly as in the turbulence investigations using much smaller geometries (see further references in e.g. [24]). Hence, the equations need to be averaged in order to obtain the mean flow (Reynolds averaging). For the system of equations to be closed, the unknown Reynolds stress term needs to be modelled in terms of mean flow variables by utilizing the Boussinesq hypothesis and a turbulence model.

Governing equations

The continuity equation is written as follows:

$$\frac{\partial \rho}{\partial t} + \nabla \cdot (\rho \vec{u}) = 0 \quad (1)$$

where $\rho, \vec{u}$ and t are density, velocity vector, and time respectively.

In the VOF approach, a single momentum equation is solved throughout the domain and the resulting velocity field is shared among the phases. Assuming turbulent flow, the momentum equation is expressed, using Reynolds averaging and the Boussinesq hypothesis, as:

$$\frac{\partial (\rho \vec{u})}{\partial t} + \nabla \cdot (\rho \vec{u}\vec{u}) = -\nabla \left(p - \frac{2}{3} k\rho \right) + \nabla \cdot \left[(\mu + \mu_t)\left(\nabla \vec{u} + \nabla \vec{u}^T \right) \right] + \rho \vec{g} + \vec{F} \quad (2)$$

where $p, \vec{g}, \mu$ and $\vec{F}$ are pressure, gravity acceleration, viscosity of the fluid and body force acting on the system, respectively. The turbulence is characterized by the turbulent kinetic energy k and the eddy viscosity μ_t.

Density and viscosity used in Eqs. (1) and (2) can be estimated as:

$$\rho = \sum_{1}^{N} \rho_q \alpha_q \quad (3)$$

$$\mu = \sum_{1}^{N} \mu_q \alpha_q \quad (4)$$

where α_q is the phase fraction of the *q*th phase. A separate continuity equation for α_q is considered as follows:

$$\frac{\partial \alpha_q}{\partial t} + \nabla \cdot \left(\alpha_q \vec{u}_q \right) = 0 \quad (5)$$

For every element, the following relationship is valid:

$$\sum_{1}^{N} \alpha_q = 1 \quad (6)$$

where *N* is the number of phases, and three conditions are possible for α_q: (1) $\alpha_q = 0$, the element does not contain the *q*th fluid; (2) $\alpha_q = 1$, the element is occupied solely by the *q*th fluid; and (3) $0 < \alpha_q < 1$, the element contains the interface between the *q*th fluid and one or more other fluids.

VOF uses a piecewise-linear method to construct the interface among fluids. It assumes that the interface between two fluids has a linear slope within every element. The scheme uses this linear shape for the calculation of the advection of fluid through the element faces. In the first step of interface reconstruction, the position of the linear interface relative to the center of every partially filled element is calculated based on the information of the volume fraction and its derivatives in the cell. After that, the advection of fluid through each face is calculated using the computed linear interface representation and information about the normal and tangential

velocity distribution on the face. Finally, the volume fraction in each cell is obtained by using the balance of fluxes calculated during the previous step [23,25,26].

Because the flow in the annular film is turbulent, whereas only the mean flow is of interest in the present study, a turbulence model is needed. The choice of turbulence model is discussed later, and the standard $k-\varepsilon$ model used herein utilizes the following two transport equations for the turbulent kinetic energy and viscous dissipation rates:

$$\frac{\partial(\rho k)}{\partial t}+\nabla\cdot(\rho k\vec{u})=\nabla\cdot\left(\left(\mu+\frac{\mu_t}{\sigma_k}\right)\nabla k\right)+2\mu_t E_{ij}E_{ij}-\rho\varepsilon \quad (7)$$

$$\frac{\partial(\rho\varepsilon)}{\partial t}+\nabla\cdot(\rho\varepsilon\vec{u})=\nabla\cdot\left(\left(\mu+\frac{\mu_t}{\sigma_\varepsilon}\right)\nabla\varepsilon\right)+C_{1\varepsilon}\frac{\varepsilon}{k}2\mu_t E_{ij}E_{ij}-C_{2\varepsilon}\rho\frac{\varepsilon^2}{k} \quad (8)$$

where k, μ_t and ε are the turbulent kinetic energy, eddy viscosity and dissipation rate respectively. k and ε are used to obtain the turbulent viscosity in the flow field through,

$$\mu_t=C_\mu\rho\frac{k^2}{\varepsilon} \quad (9)$$

and they are together with k used in the momentum equation (2).

E_{ij} used above is defined as

$$E_{ij}=\frac{1}{2}\left(\frac{\partial u_i}{\partial x_j}+\frac{\partial u_j}{\partial x_i}\right) \quad (10)$$

The constants are taken as C_{μ} = 0.09, σ_k = 1.00, σ_{ε} = 1.30, $C_{1\varepsilon}$ = 1.44, and $C_{2\varepsilon}$ = 1.92 [23].

Surface tension and wall adhesion

The VOF model also includes the efforts of surface tension along the interface between every pair of phases. The surface tension model uses the continuum surface stress (CSS) model proposed by Lafaurie et al [27]. In this model, the surface tension force is represented as

$$F_{CSS} = \nabla \cdot \left[\sigma \left(|\nabla \alpha| I - \frac{\nabla \alpha \otimes \nabla \alpha}{|\nabla \alpha|} \right) \right] \quad (11)$$

where I is the unit tensor, σ is surface tension coefficient, and $\otimes$ is tensor product of the two vectors: the original normal and the transformed normal.

The CSS method does not require any explicit calculation for the curvature, so it performs better than other models in under-resolved regions [25]. In this study, the oil-water annular flow in U-bend contains heavy oil/water/pipe wall surface, hence the surface tension between oil and water is described using a surface tension coefficient while the surface tension between fluid and pipe wall is described by the contact angle.

The hydrodynamic parameters

(1) Mixture Reynolds number, Re_m

$$\mathrm{Re}_m = D u_m \rho_m / \mu_m \quad (12)$$

where D is diameter of bend pipe; u_m is mixture velocity, and $u_m = u_{so} + u_{sw}$, u_{so} and u_{sw} are superficial velocity of lube oil and water respectively; and ρ_m is mixture density,

$\rho_m = \frac{\rho_o u_{so}}{u_{so} + u_{sw}} + \frac{\rho_w u_{sw}(1.35 u_{so} + u_{sw})}{(u_{so} + u_{sw})^2}$, μ_m is mixture viscosity.

(2) The equivalent two-phase loss coefficient, k_{tp}

$$k_{tp} = 2\Delta P_{hydro} / (\rho_m u_m^2) \quad (13)$$

where ΔP_{hydro} is hydrodynamic pressure drop.

(3) The area-weighted average of oil volume fraction, α_o

$$\alpha_o = \frac{1}{A}\sum_{i=1}^{n} \alpha_{oi} A_i \quad (14)$$

where A_i and A are the area occupied by oil and the area of cross-section respectively.

(4) Fouling characteristics, φ_f

Fouling could lead to severe problem during transportation of heavy oils. From the experiments of Sharma et al. [22] it was observed that fouling could occur at the bend under specific operating conditions. The point at which the water film adheres to the pipe wall is considered as

the initiation point of fouling. Geometrically, this point has been defined as the corresponding angle of the bend (φ_f) by Sumana et al. [23], and is reproduced in Fig. 1a for convenience.

SIMULATION SYSTEM AND NUMERICAL PROCEDURE

Simulation system

A three-dimensional model has been developed to analyze U-bend core annular flows. Fig. 1b schematically depicts the flow geometry. A tube of diameter (D) 0.012m is in the form of a U bend, whose radius is 0.1m, and the curvature ratio (2R/D) is 16.67. D1 is oil inlet diameter, and its initial value is 0.008m. For comparing the variation of flow parameters, five sections in computational domain are selected for the analysis. In order to establish the core annular flow, co-axial entry of both the fluids with lube oil ($\rho_o = 960 kg/m^3$ and $\mu_o = 0.22 Pa \cdot s$) at the center, and water ($\rho_w = 998.2 kg/m^3$ and $\mu_w = 0.001003 Pa \cdot s$) at the annular area has been considered as shown in Fig. 1b.

The computational fluid dynamics software package FLUENT 14.5 has been used for the simulation. The governing equations are discretized using the finite volume technique. After discretization, the equations are solved using a segregated solver. The computation has been done for unsteady flow to investigate the initial development of core annular flow. This simulation is based on the assumptions of immiscible liquid pair, constant liquid properties and co-axial entry of the liquids instead of the converging entry as in real cases.

Meshing of the model

The mesh generation in the computational domain has been done using software ANSYS Workbench. The meshed geometry and the mesh in the cross-section are shown in Fig. 2. There are 72816 hexahedral elements and 79373 nodes. The mesh independence test has been performed and the equivalent two-phase loss coefficient (k_{tp}) does not change much when the number of cells is decreased from 223245 to 72816 (Fig. 3), hence the final grid of 72816 elements is sufficiently accurate, and is used to save computational time.

Boundary conditions

In the following the subscript *x* denotes the axial direction, *r* denotes the radial direction while oil (o) and water (w) refer to oil phase and water phase respectively (see Fig. 1b).

(1) Inlet boundary condition. The oil velocity is specified at the core area and water velocity at the annular area. Considering uniform velocity distribution, the initial conditions are:

At $0 \le r \le D1$, $u_x = u_o$, the turbulence specification method is intensity and hydraulic diameter, here backflow turbulent intensity is 5% and backflow hydraulic diameter is 0.008m;

At $D1 < r \le D$, $u_x = u_w$, the backflow turbulent intensity is 5% and backflow hydraulic diameter is 0.002m.

(2) Wall boundary conditions. A stationary, no-slip ($u_x = 0$), no penetration ($u_r = 0$) boundary is imposed on the wall of the pipe. In addition, a contact angle (27°) between water and pipe wall material (acrylic resin) is provided at the wall.

(3) Outlet boundary condition. A pressure outlet boundary is set on the pipe, the backflow turbulent intensity is 5% and backflow hydraulic diameter is 0.012m.

Discretization methods and convergence criterion

Owing to the dynamic nature of the two-phase flow, a transient simulation with a time step of 0.001 s is carried out. Different methods of discretization of the governing equations are used. PRESTO (PREssure STaggering Option) [28] scheme is used for continuity equation and a second order upwind scheme is used for momentum, while a first order upwind method is used for turbulent kinetic energy and dissipation rate. The pressure-velocity coupling is implemented via the SIMPLE (Semi-Implicit Method for Pressure Linked Equation) [29] algorithm.

The convergence criteria are set based on the residual value of the calculated variables namely mass, velocity components and volume fraction. In this study, the convergence criterion for all variables is chosen to be 10^{-3}.

VALIDATION

For the purpose of validating the simulation, the results are compared with the experimental data for the equivalent two-phase loss coefficient k_{tp}, as reported by Sharma et al. [22]. Fig. 3 depicts a few representative simulated results of the equivalent two-phase loss coefficient along with the corresponding results as obtained from experiments. In the figure, the numerical simulations are close to the experimental results, with the error in the range of 5%. These differences as compared with the experimental data come from the numerical error, model error, etc.

Furthermore, the development of oil-water core annular flow is shown in Fig. 4, which depicts the cross-sectional contours of oil volume fraction (oil phase distribution) at the five sections at different time instants for oil superficial velocity, u_{so} = 0.6 m/s and water superficial velocity, u_{sw} = 0.4 m/s. The figure clearly denotes that the core flow at the cross-section 2-4 is eccentric in nature. It also reveals the 3D feature of the interfacial configuration and the fouling phenomena.

RESULTS AND DISCUSSION

After validation with experiments, a number of studies have been conducted with a variation of parameters and models, including turbulence models, oil properties (the physical properties of oil are listed in Table 1 [22, 30, 31]), different inclination angle, varied inlet diameter ratio, and various pipe materials. Additional information on the hydrodynamics of core annular flow is

obtained. These results could help us understand the influence of these above mentioned factors on the hydrodynamics and the fouling.

The effect of turbulence model

In order to select appropriate turbulence model for this calculation, various models including standard $k-\varepsilon$, standard $k-\omega$, SST (Shear-Stress Transport) $k-\omega$, RNG (ReNormalization Group) $k-\varepsilon$, Realizable $k-\varepsilon$ are tested and results are shown in Fig. 5. All the turbulent models provide the similar prediction of oil volume fraction, so the standard $k-\varepsilon$ model is used in this study. This model is based on model transport equations for the turbulence kinetic energy (k) and its dissipation rate (ε). In fact, from the reference [25], the standard k-ε model is more robust, has better economy (the simulation time is shorter), and possesses reasonable accuracy for a wider range of turbulent flows than other turbulence models. On the other hand, the standard $k-\omega$ model is based on the transport equations for the specific dissipation rate and has proven superior in flows involving separation of turbulent boundary layers. The variants of $k-\varepsilon$ and $k-\omega$ models listed above have been developed to improve the turbulence modelling in various flow conditions. All the models tested are based on the eddy-viscosity concept, where the turbulence is essentially modelled as an additional viscosity.

The effect of oil property

Subsequently, the studies have been directed to understand the variation of α_o, k_{tp}, and φ_f with oil properties. In this case, u_{so} is remained constant at 0.6m/s and u_{sw} is varied from 0.4 to 0.9 m/s, so that Re_m becomes a function of u_{sw} only. In Fig. 6a, α_o is plotted for different oil properties and, clearly, α_o decreases with increasing Re_m for all cases. Furthermore, due to the highest viscosity of fuel oil, α_o is lower for the other oils under all velocity conditions. Hence, the tendency is that the higher viscosity the lower α_o. To understand the reason behind this, we can combine with the contours in Fig. 6b, which shows the all oil phase fraction contours at cross-section 1 and cross-section 5 under $Re_m \approx 10683$. It is evident that oil with low density or low viscosity implies a low dynamic pressure loss, and can hence easily be carried downstream.

Fig. 6c depicts the influence of the oil property on k_{tp}. For oils of same density, k_{tp} decreases as the viscosity increases, such as lube oil and fuel oil. In order to further understand the variation of k_{tp} with oil property, the oil phase distribution in Fig. 6b is considered. From these distributions, as oil-water flow through the U-bend, the oil breaks the water film to adhere onto the pipe wall. The fouling surface of lube oil is larger than that of fuel oil or crude oil, which in turn leads to greater k_{tp}. However, the fouling surface of Troika oil is larger than that of lube oil, hence k_{tp} is lower than that of lube oil due to its viscosity is only one-tenth of that of lube oil. Also Fig. 6c reveals that k_{tp} decreases with lower oil density and viscosity. For all

cases, k_{tp} decreases with an increase in Re_m, this tendency agrees with the experimental results of Sharma et al. [22].

The influence of oil property on fouling point is represented in Fig. 6d. From this figure, it can be concluded that viscosity plays a key role for φ_f . Greater viscosity leads to lower fouling trend, i.e. the oil remains in the core region longer when its viscosity is larger -- which is also clearly seen in Fig. 6b. Oliemans [32] studied the feasibility of core annular flow as a function of oil viscosity, noting that the higher the oil viscosity the easier is the formation of core annular flow, with the explanation that it is difficult for the high viscosity oil to rupture the water film which adheres to the bend wall, and hence φ_f becomes large.

The effect of inclination angle

Slightly inclined U-bend installations are common phenomena in petroleum industry. Mukherjee et al. [33] studied that the effect of the inclination angles on water holdup and friction pressure. Sumana et al. [23] simulated the influence of different flow direction on pressure ratio and fouling characteristics. However, they only simulated the upflow, downflow and horizontal flow. In this study, the inclined upflow is considered, as shown in Fig. 7.

To investigate the effect of inclination angle on α_o, k_{tp}, and φ_f, the inclination angle is varied in the range from 0 to 30^o downward, and the results are shown in Fig. 7. Fig. 7a reveals

that α_o increases gradually with the increasing inclination angle. This is due to the gravity in flow plane which reduces along with the increasing inclination angle.

It is noted from Fig. 7b that the reduction of k_{tp} with increased inclination angle is more pronounced as the inclination angle is varied from 0 to 10^o, the probable reason being the influence of the change of the gravity component. The contours of four points in Fig. 7c can help us understand the reason for that k_{tp} varies with inclination angle. As noted in Fig. 7b, from point I to II, or from point III to IV, the surface of oil adhering to pipe wall decreases with increasing inclination angle, which consequently leads to lower k_{tp}.

Fig. 7d depicts the relationship of φ_{f} and inclination angle, and clearly φ_{f} decreases with the increasing inclination angle. As explained before, when the inclination angle increases, the gravity in the flow plane decreases, and the aqueous film is easily broken owing to the action of the centrifugal force.

The effect of inlet diameter ratio

For this investigation, the inlet diameter ratio (D1/D, D1 is oil inlet diameter, D is the diameter of the pipe) is varied from 0.583 to 0.833, while D is kept unaltered at 0.012m. An effort to study the influence of inlet diameter ratio on α_o, k_{tp}, and φ_{f} is conducted, and the results are shown in Fig. 8. Fig. 8a gives the variation of α_o with inlet diameter ratio. It can be seen that α_o increases gradually as the inlet diameter ratio (D1/D) increases. It is evident that as the

diameter ratio increases, the area of oil in the inflow cross section increases, and the volume fraction of oil increases. The phase distribution contours at cross-section 1 and cross-section 5 are depicted in Fig. 8b, showing that the fouling is occurring downstream (in cross section 5). From the phase distribution contours at cross-section 1 for points I-IV, α_o increases with an increase in D1/D. Note that points IV and V represent identical D1/D. However, due to the decrease of oil with an increase in Re_m [34], α_o in point IV is greater than that in point V.

The impact of inlet diameter ratio (D1/D) on k_{tp} is investigated next, and is shown in Fig. 8c. It is evident from the figure that k_{tp} decreases with increase in diameter ratio (D1/D) for different Re_m for small values of D1/D. For D1/D above 0.75, k_{tp} increases with larger D1/D, the reason being that as D1/D increases, the area of oil increases and the oil flow resistance increases as well, hence k_{tp} increases. From the phase contours in Fig. 8b, the oil-water flow crosses the U-bend, the oil sticks onto the pipe wall, and leads to the hydrodynamic pressure drop. The fouling surface plays a role in determining the magnitude of k_{tp}; more fouling surface results in higher k_{tp}. This can help us understand the variation of k_{tp} with inlet diameter ratio.

The variation of φ_f with diameter ratio is shown in Fig. 8d. The figure shows that φ_f increases until it attains a maximum value and then decreases with increasing diameter ratio for all given oil and water superficial velocity. The reason is that as the area of water inlet reduces, the annular water film becomes thinner, and then the oil could break the water film and adhere on the bend wall.

The effect of pipe materials

Further attempts have been conducted to understand the impact of pipe material on α_o, k_{tp}, and φ_f. There are four pipe materials in this study, namely, the carbon steel (CS), galvanized steel (GS), stainless steel (SS), borosilicate glass (BG). Their contact angles are 156°, 154°, 149°, and 104° respectively. These contact angles are from reference [35], and are contact angles of oil and different material surfaces immersed in pure water; and the original crude oil (density 940 kg/m^3, viscosity 0.511 Pa·s, surface tension 0.0331 N/m) is used. The different contact angles between water and pipe wall are introduced into FLUENT 14.5 as wall boundary conditions, and the results are shown in Fig. 9.

Fig. 9a indicates that pipe material slightly influences α_o which increases slowly with increasing contact angle. The reason may be that as the contact angle increases, the wettability of oil to pipe wall increases, and induces a larger wetting force, which leads to an increase in α_o.

k_{tp} is affected by pipe material variation as can be observed in the graph of Fig. 9b. k_{tp} increases with increasing contact angle. To find out the reason behind this, the cross-sectional contours of phase fraction at the section 1 and section 5 of the U-bend for four different contact angles under $\mathrm{Re}_m \approx 9489$ (u_{so} = 0.6 m/s and u_{sw} = 0.8 m/s) are plotted in Fig. 9c. From these contours, the surface of oil sticking to pipe wall increases with the increase contact angle, which leads to a higher pressure loss ratio.

From Fig. 9d it is observed that φ_f increases with increasing contact angle. For this reason, the hydrophilic material (with low contact angle) is better for reducing the fouling tendency.

CONCLUSIONS

The present work investigates the influence of the oil property, the inclination angle, the inlet diameter ratio and the pipe material on α_o, k_{tp}, and φ_f. The numerical simulation results presented are expected to be useful for designing pipeline networks. Through numerical simulation, it is found that the fouling surface plays a role in determining the magnitude of k_{tp}. A large fouling surface, can result in high values of k_{tp}. As the viscosity difference between two fluids increases, the two-phase flow remains a core annular flow as it flows through the U-bend. Hence, a mixture flow of high viscosity oil and water could reduce the chance of fouling when it flows through the U-bend. As the inclination angle of the U-bend increases, α_o increases, k_{tp} and φ_f decrease. Thus, the upflow with a small inclination angle of oil-water mixture through a U-bend is preferable. If the inlet diameter ratio (D1/D) is increased, the area of water inlet decreases, which leads to low values of α_o, k_{tp} and φ_f. For this reason, if the inlet diameter ratio is in the range of 0.6-0.75, the oil-water two-phase may experience a more stable core annular flow across the U-bend. Furthermore, the pipe material influences α_o, k_{tp} and φ_f, and a pipe with hydrophilic behavior reduces the fouling tendency.

ACKNOWLEDGEMENT

The authors gratefully acknowledge research support from the Agency for Science, Technology and Research (A*STAR) and Engineering Research Grant, SERC Grant No: 1021640147.

NOMENCLATURE

A_i	area occupied by oil, m^2
A	area of the cross-section, m^2
BG	borosilicate glass
CS	carbon steel
CSS	continuum surface stress
C_μ	constant
$C_{1\varepsilon}$	constant
$C_{2\varepsilon}$	constant
D	pipe diameter, m
D1	diameter of oil inlet, m
E_{ij}	mean strain rate tensor, 1/s
F	body force, kg/m^2s

g	gravitational constant, m/s^2
GS	galvanized steel
I	unit tensor
k	turbulent kinetic energy, m^2/s^2
k_{tp}	equivalent two-phase loss coefficient
N	number of phases
Nu	cell number
p	pressure in the flow field, Pa
ΔP_{hydro}	hydrodynamic pressure drop, Pa
r	radial direction
R	radius of curvature of the bend, m
Re_m	mixture Reynolds number
SS	stainless steel
t	time, s
$\vec{u}$	velocity vector, m/s

u_m	mixture velocity, m/s
u_o	oil velocity, m/s
VOF	volume of fluid
u_r	radial velocity, m/s
u_{so}	superficial oil velocity, m/s
u_{sw}	superficial water velocity, m/s
u_x	axial velocity, m/s
u_w	water velocity, m/s
x	axial direction
z	z direction

Greek symbols

α	phase fraction
ε	dissipation rate, m^2/s^3
μ	viscosity, Pa-s
μ_t	eddy viscosity, Pa-s

μ_m	mixture viscosity, Pa-s
φ_f	angle of the bend at fouling point, ^{o}
ω	specific dissipation rate, 1/s
ρ_m	mixture density, kg/m^3
σ	surface tension coefficient, N/m
σ_k	constant
σ_ε	constant

Subscripts

q phase order

m mixture

w water

o oil

REFERENCES

[1] Charles, M.E., Govier, G.W., and Hodgson, G.W., The horizontal pipeline flow of equal density of oil-water mixtures, *Canadian Journal of Chemical Engineering*, vol. 39, pp. 17-36, 1961.

[2] Arney, M.S., Bai, R., Guevara, E., Josenph, D.D., and Liu, K., Friction factor and hold up studies for lubricated pipelining-1. Expeiments and correlations, *International Journal Multiphase Flow*, vol. 19, pp. 1061-1067, 1993.

[3] Sotgia, G., Tartarini, P., and Stalio, E., Experimental analysis of flow regimes and pressure drop reduction in oil-water mixtures, *International Journal Multiphase Flow*, vol. 34, pp. 1161-1171, 2008.

[4] Parda, V.J.W., and Bannwart, A.C., Modeling of vertical core-annular flows and application to heavy oil production, *Journal of Energy Resources Technology*, vol. 123, pp. 194-199, 2001.

[5] Rodriguez, O.M.H., Bannwart, A.C., and Carvalho, C.H.M., Pressure loss in core annular flow: modeling, experimental investigation and full scale experiments, *Journal of Petroleum Science and Engineering*, vol. 65, pp. 67-75, 2009.

[6] Bai, R., Kelkar, K., and Joseph, D.D., Direct simulation of interfacial waves in a high viscosity ratio and axisymmetric core annular flow, *Journal of Fluid Mechanic*, vol. 327, pp. 1-24, 1996.

[7] Kao, T., Choi, H.G., Bai, R., and Joseph, D.D., Finite element method simulation of turbulent wavy core-annular flows using a *k-w* turbulence model method, *International Journal Multiphase Flow*, vol. 28, pp. 1205-1222, 2002.

[8] Myungoo, K., Hyeseon, S., Stanley, O., Level set based simulations of two-phase oil-water flows in pipes, *Journal of Scientific Computing*, vol. 31, pp. 153-184, 2007.

[9] Chisholm,vD., Two-phase flow in bends, *International Journal Multiphase Flow*, vol. 6, pp. 363-367, 1980.

[10] Chen, I.Y., Wang, C.C., and Lin, S.Y., Measurements and correlations of frictional single-phase and two-phase pressure drops of R-410A flow in small U-type return bends, *International Journal of Heat and Mass Transfer*, vol. 47, pp. 2241-2249, 2004.

[11] Chen, I.Y., Wu, Y.S., Liaw, J.S., and Wang, C.C., Two-phase frictional pressure drop measurements in U-type wavy tubes subject to horizontal and vertical arrangements, *Applied Thermal Engineering*, vol.v28, pp. 847-855, 2008.

[12] Huang, M., Yang, Z., Duan, Y.Y., and Lee, D.J., Bubble growth for boiling bubbly flow for R141B in a serpentine tube, *Journal of the Taiwan Institute of Chemical Engineers*, vol. 42, pp. 727-734, 2011.

[13] Kerpel, K.D., Ameel, B., Huisseune, H., Joen, C.T., Caniere, and H., Paepe, M.D., Two-phase flow behavior and pressure drop of R134a in a smooth hairpin, *International Journal of Heat and Mass Transfer*, vol. 55, pp.1179-1188, 2012.

[14] Usui, K., Aoki, S., and Inoue, A., Flow behavior and pressure drop of two-phase flow through C-shaped bend in vertical plane – (i) upward flow, *Journal of Nuclear Science and Technology*, vol. 17, pp. 875-887, 1980.

[15] Usui, K., Aoki, S., and Inoue, A., Flow behavior and phase distribution in two-phase flow around inverted U bend, *Journal of Nuclear Science and Technology*, vol. 20, pp. 915-928, 1983.

[16] Chen, I.Y., Yang, Y.W., and Wang, C.C., Influence of horizontal return bend on the two-phase flow pattern in 6.9 mm diameter tubes, *Canadian Journal of Chemical Engineering*, vol. 82, pp. 478-484, 2002.

[17] Wang, C.C., Chen, I.Y., and Shyu, H.J., Frictional performance of R-22 and R-410A inside a 5.0 mm wavy diameter tube, *International Journal of Heat and Mass Transfer*, vol.46, pp.755-760, 2003.

[18] Wang, C.C., Chen, I.Y., and Huang, P.S., Two-phase slug flow across small diameter tubes with the presence of vertical return bend, *International Journal of Heat and Mass Transfer*, vol.48, pp. 2342-2346, 2005.

[19] Wang, C.C., Chen, I.Y., Lin, Y.T., and Chang, Y.J., A visual observation of the air-water two-phase flow in small diameter tubes subject to the influence of vertical return bend, *Chemical Engineering Research and Design*, vol. 86, pp. 1223-1235, 2008.

[20] Abdulkadir, M., Zhao, D., Azzi, A., Lowndes, I.S., and Azzopardi, B.J., Two-phase air-water flow through a large diameter vertical 180^{o} return bend, *Chemical Engineering Science*, vol. 79, pp. 138-152, 2012.

[21] Sharma, M., Ravi, P., Ghosh, S., Das, G., and Das, P.K., Studies on low viscous oil–water flow through return bends, *Experimental Thermal and Fluid Science*, vol. 35, pp. 455-469, 2011.

[22] Sharma, M., Ravi, P., Ghosh, S., Das, G., and Das, P.K., Hydrodynamics of lube oil-water flow through 180^{o} return bends, *Chemical Engineering Science*, vol. 66, pp. 4468-4476, 2011.

[23] Sumana, G., Das, G., and Das, P.K., Simulation of core annular in return bends-A comprehensive CFD study, *Chemical Engineering Research and Design*, vol. 89, pp. 2244-2253, 2011.

[24] Skote, M., Scaling of the velocity profile in strongly drag reduced turbulent flows over an oscillating wall, *International Journal of Heat and Fluid Flow,* vol. 50, pp. 352-358, 2014.

[25] Fluent 14.5 User's Guide, Ansys Inc., Canonsburg, USA, 2012.

[26] Jiang, F., Wang, Y.J., Ou, J.J., and Xiao, Z.M., Numerical simulation on oil-water annular flow through the Ⅱ bend. *Industrial & Engineering Chemistry Research,* vol. 53, pp. 8235-8244, 2014.

[27] Lafaurie, B., Nardone, C., Scardovelli, R., Zaleski, S., and Zanetti, G., Modelling merging and fragmentation in multiphase flows with SURFER, *Journal of Computational Physics,* vol.113, pp. 134-147, 1994.

[28] Patankar, S.V., Numerical heat transfer and fluid flow, Hemisphere, Washington, DC, 1980.

[29] Hanif, M., Markus, B., and Javad, M., Accurate implementation of forcing terms for two-phase flows into SIMPLE algorithm, *International Journal Multiphase Flow,* vol. 45, pp. 40-52, 2012.

[30] Roudsari, S.F., Turcotte, G., Dhib, R., and Farhad, E.M., CFD modeling of the mixing of water in oil emulsions, *Computers & Chemical Engineering,* vol. 45, pp.124-136, 2012.

[31] Bannwart, A.C., Rodriguez, O.M.H., Carvalho, C.H.M., Wang, I.S., and Vara, R.M.O., Flow patterns in heavy crude oil-water flow, *Journal of Energy Resources Technology*, vol. 126, pp. 184-189, 2004.

[32] Oliemans, R.V.A., The lubricating-film model for core-annular flow, Ph.D. Thesis, Delft University of Technology, The Netherlands, 1986.

[33] Mukherjee, H., Brill, J.P., and Beggs, H.D., Experimental study of oil–water flow in inclined pipes, *Journal of Energy Resources Technology,* vol. 103, pp. 56-66, 1981.

[34] Ghosh, S., Das, G., and Das, P.K., Simulation of core annular downflow through CFD-A comprehensive study. *Chemical Engineering Progress,* vol. 49, pp. 1222-1228, 2010.

[35] Santos, R.G., Rahoma, S.M., Bannwart, A.C., and Loh, W., Contact angle measurements and wetting behavior of inner surfaces of pipelines exposed to heavy crude oil and water, *Journal of Petroleum Science and Engineering,* vol. 51, pp. 9-16, 2006.

Table 1 Physical properties of different oil.

Oil name	Density (kg/m^3)	Viscosity (Pa.s)	Surface tension (N/m)
Lube oil [22]	960	0.22	0.039
Troika oil [30]	869	0.02	0.011
Fuel oil [31]	960	18	0.03
Crude oil [31]	925	0.5	0.029

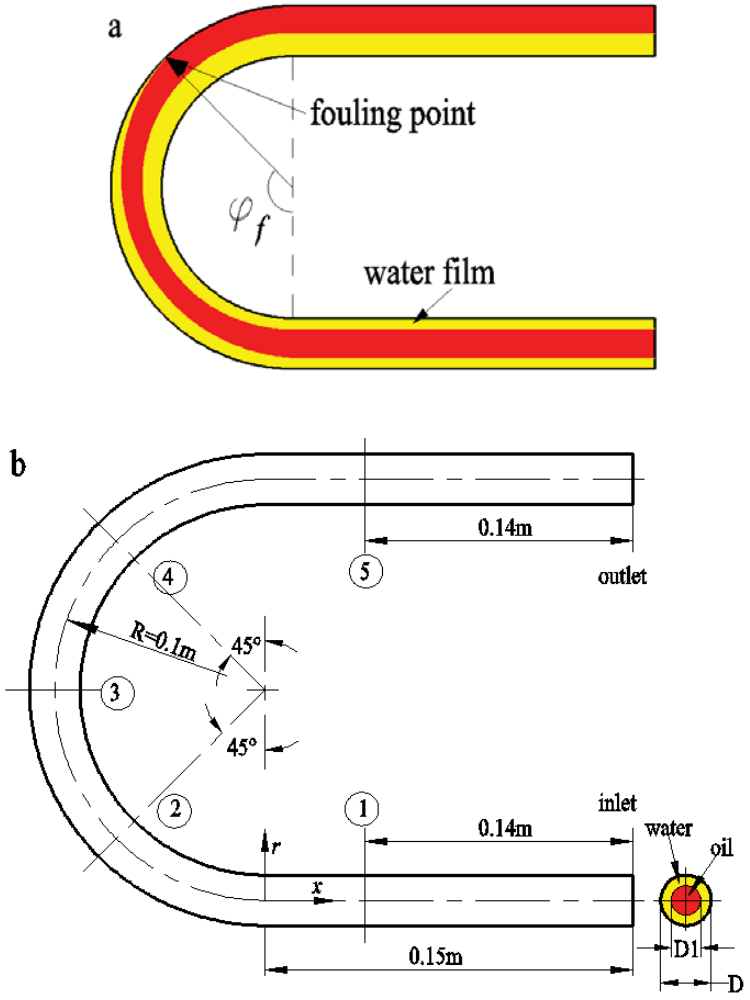

Fig. 1 The U-bend. (a) Fouling point at bend; (b) schematic of model geometry. oil, water.

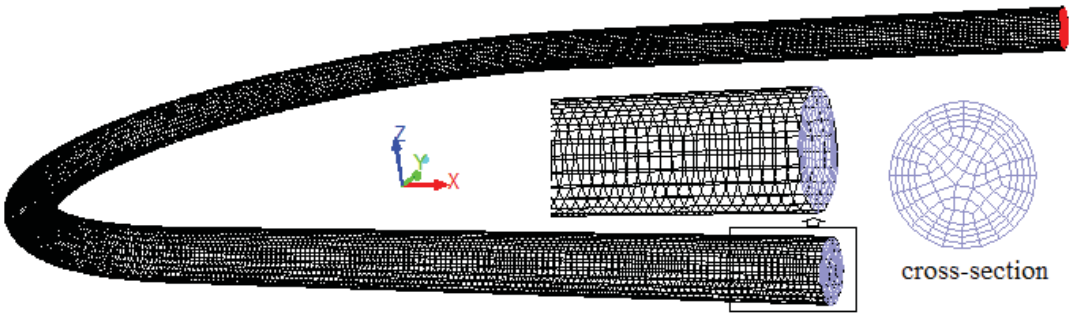

Fig. 2 The meshed geometry.

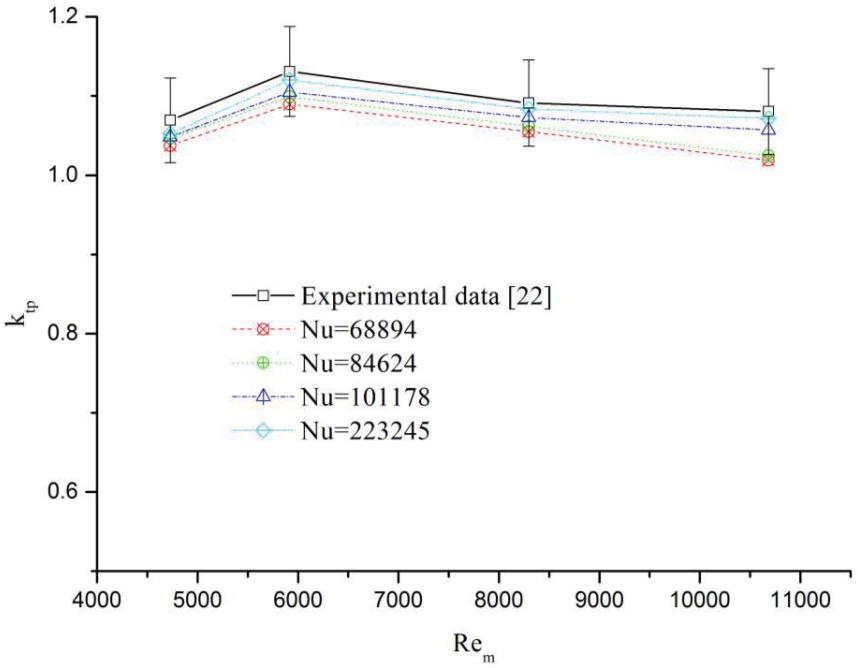

Fig. 3 Comparison of numerical and experimental results (Sharma et al. [22]). Nu is the cell number. The error bars illustrate the 5% limits around the experimental data.

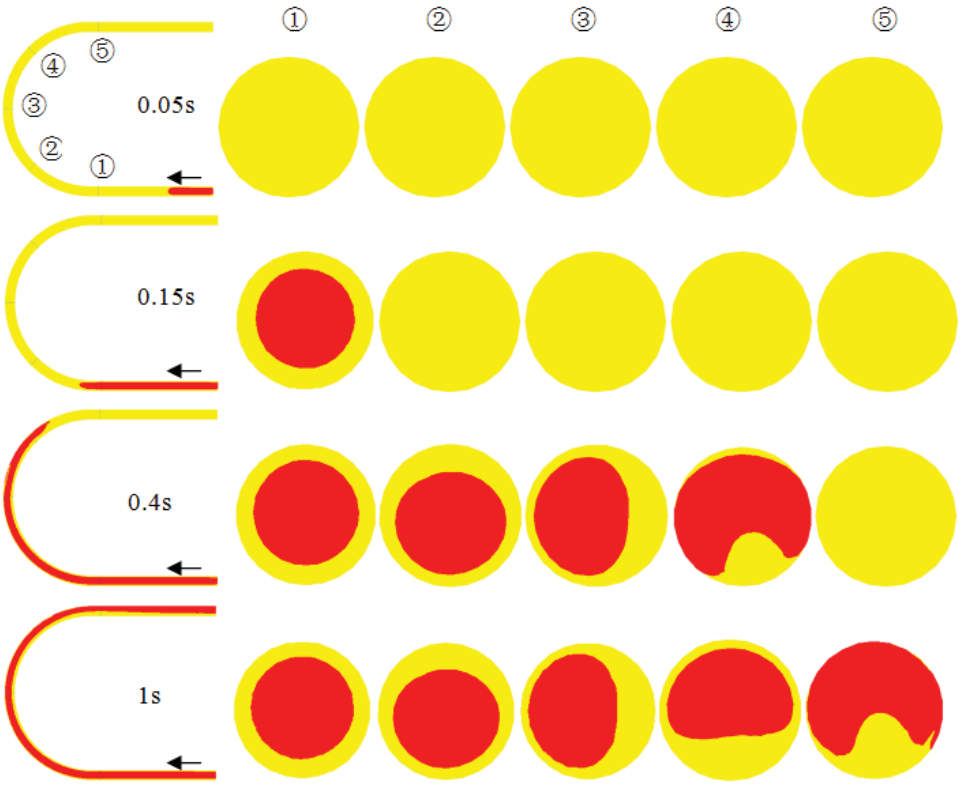

Fig. 4 Development of core flow at section 1- section 5 during upflow through U bend; v_{so} = 0.6 m/s, v_{sw} = 0.4 m/s; oil, water.

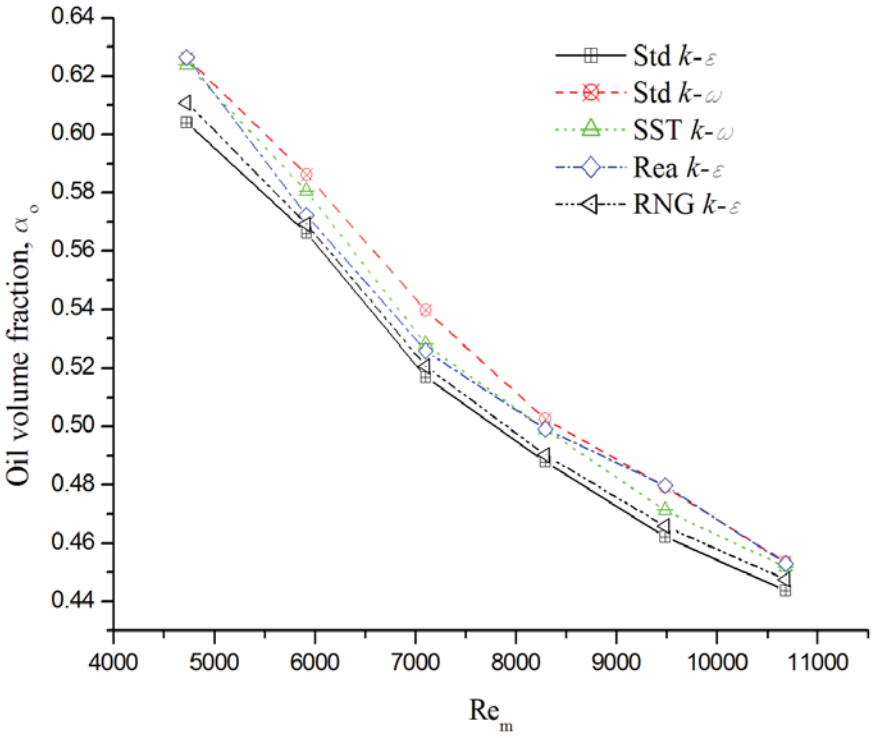

Fig. 5 Comparison between different turbulence models.

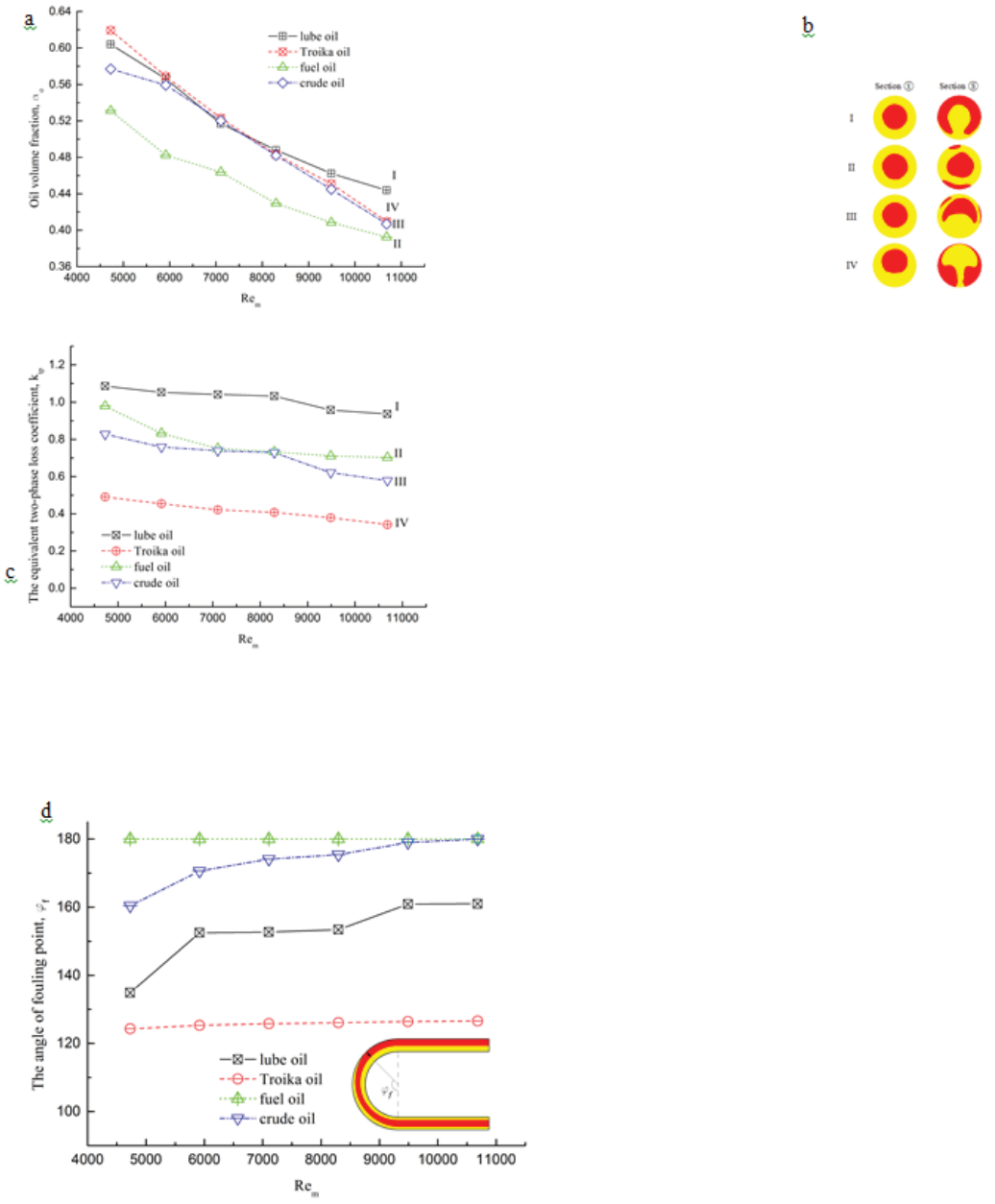

Fig. 6 The influence of oil property. (a) Variation of α_o with different oil property; (b) the oil phase fraction contours at points of I-IV; (c) variation of k_{tp} with different oil property; (d) variation of φ_f with different oil property.

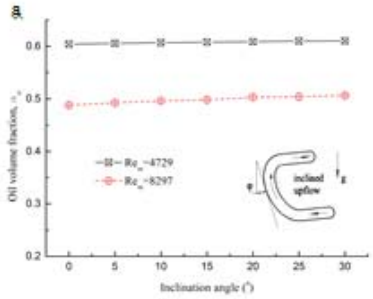

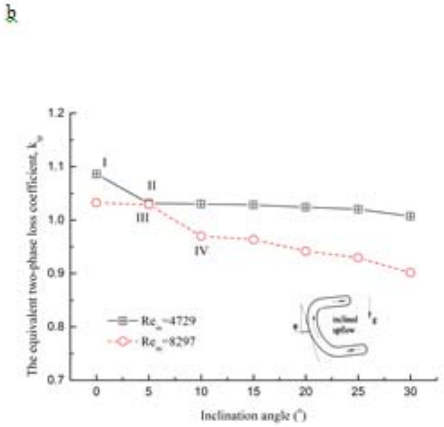

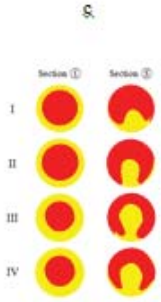

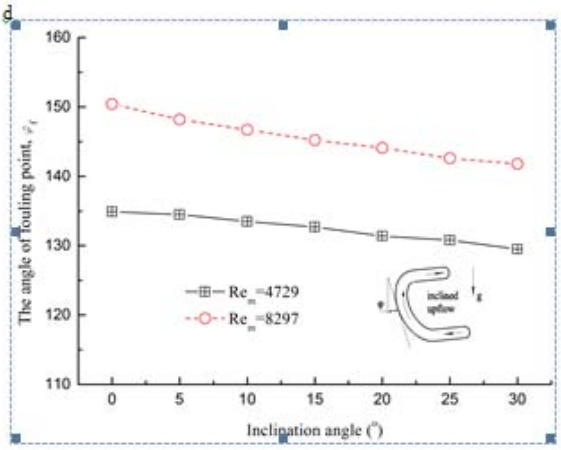

Fig. 7 The influence of inclination angle. (a) Variation of α_o with different inclination angle; (b) variation of k_{tp} with different inclination angle; (c) the phase fraction contours at points of I-IV; (d) variation of φ_f with different inclination angles.

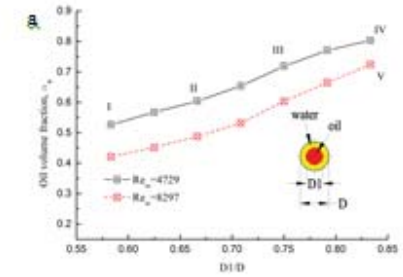

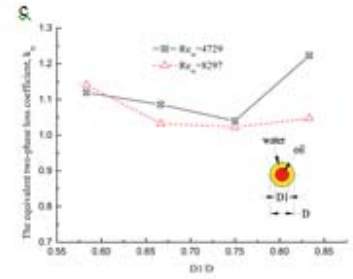

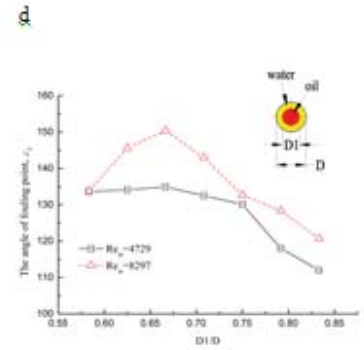

Fig. 8 The influence of inlet diameter ratio. (a) Variation of α_o with inlet diameter ratio; (b) the phase fraction contours at points I-V; (c) variation of k_{tp} with inlet diameter ratio; (d) variation of φ_f with inlet diameter ratio.

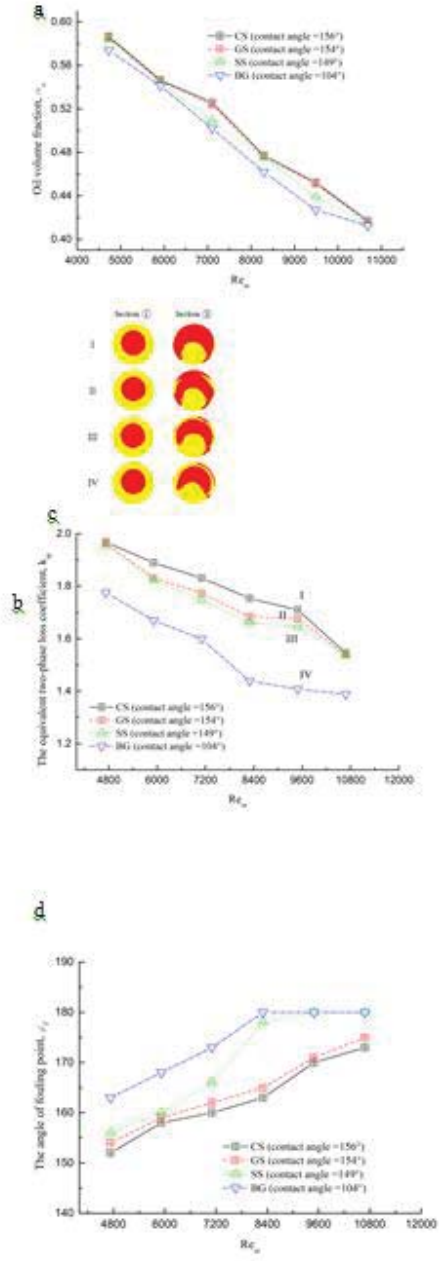

Fig. 9 The influence of pipe material. (a) Variation of α_o with contact angle; (b) variation of k_{tp} with contact angle; (c) the contours at points of I-IV; (d) variation of φ_f with contact angle.